

Electronic Supporting Information:

Molybdenum-decorated V_2O_5 - WO_3 / TiO_2 : Surface engineering toward boosting the acid cycle and redox cycle of NH_3 -SCR

Ziyi Chen, Xiaomin Wu, Kaiwen Ni, Huazhen Shen, Zhiwei Huang, Zuoming Zhou and Guohua Jing*

Department of Environmental Science & Engineering, College of Chemical Engineering, Huaqiao University, Xiamen, Fujian 361021, China

*Corresponding authors. Tel.: +86-0592-6162300.

E-mail: zhoujing@hqu.edu.cn

Characterization

XRD patterns of the samples were obtained with a Bruker D8 Advance X-ray diffractometer with scan rate of 5°/min in the range from 20° to 80°. The BET method was used to measure the specific surface areas of the catalysts. The morphology of the catalyst was observed by SEM with a Hitachi SU8020. A FEI Tecnai G20 instrument was used to collect TEM and HRTEM images at an accelerating voltage of 200 kV. XPS experiments were performed with a Thermo Scientific Escalab 250Xi electron spectrometer, calibrated by the C 1 s peak at a binding energy (B.E.) of 284.6 eV. ICP data were collected by an iCAPQ6300 (Thermo Fisher). Raman experiments were carried out on a HORIBA HR Evolution spectrometer equipped with an optical microscope at room temperature. Dehydrated-Raman spectra were recorded at 250 °C in a feed gas of O₂/He (5 vol.%H₂/N₂) with a flow rate of 60 mL/min after dehydration pretreatment at 400 °C for 0.5 h. ⁵¹V NMR experiments were performed on a Bruker AVANCE III 600 spectrometer operating at a frequency of 157.8 MHz. Spectra were obtained from 35000 scans with a 0.3 s recycle delay in a spectral width of 1 MHz.

H₂-TPR and NH₃-TPD were conducted on a Quantachrome AutoSorb IQ-C-TCD-MS analyzer and Micromeritics Autochem 2920, respectively. For H₂-TPR, the sample (100 mg) was pretreated with a flow of He for 30 min at 300 °C. After cooling to room temperature, the sample was heated with a ramp of 10 °C/min in flowing H₂ (5 vol.% H₂/N₂) with a flow rate of 50 mL/min. The temperature was increased from 30 °C to 1000 °C. For NH₃-TPD, the sample (100 mg) was pretreated for 30 min at 300 °C in a flow of highly purified He. After cooling to room temperature, the sample was exposed to NH₃ (1 vol% NH₃/He) with a flow rate of 100 mL/min for 1 h at 30 °C, followed by purging with pure He to remove gaseous NH₃ and physically adsorbed NH₃. Finally, NH₃ desorption took place in a 100 mL/min flow of He with heating rate of 10 °C/min from 30 °C to 800 °C.

In situ DRIFTS spectra were collected on a Nicolet 6700 FTIR spectrometer equipped with a high-temperature reaction cell. Before each test, the catalyst was pretreated in flowing N₂ for 30 min at 400 °C. Subsequently, the temperature was cooled to 250 °C, and background spectra subtracted from the sample spectrum was recorded for each measurement. All spectra were recorded by accumulating 64 scans at a 4 cm⁻¹ resolution.

Catalytic Evaluation

The NH₃-SCR activity was analyzed with a continuous fixed-bed quartz reactor (i.d. = 6 mm) at atmospheric pressure. The program temperature ranged from 100°C to 400 °C. In each test, the catalyst was sieved to 40-60 mesh first, and then 0.5 g of sample was fixed on quartz wool in the middle of the reactor. Gaseous N₂ was used as the carrier gas, and the feed gas contained NO (600 ppm), NH₃ (600 ppm), O₂ (6.0 vol.%), SO₂ (100 ppm when used) and H₂O (5.5% when used). The gas hourly space velocity (GHSV) was 51000 h⁻¹ and the total flow rate was 600 mL/min. The concentrations of NO, NO₂, N₂O and NH₃ at the inlet and outlet were measured by a gas analyzer (Testo 350, Germany). The calculation equations of NO conversion and N₂ selectivity are as follows:

$$\text{NO conversion (\%)} = \left(1 - \frac{[\text{NO}]_{\text{out}}}{[\text{NO}]_{\text{in}}}\right) \times 100\% \quad (1)$$

$$\text{N}_2 \text{ selectivity (\%)} = \left(1 - \frac{[\text{NO}_2]_{\text{out}} + 2[\text{N}_2\text{O}]_{\text{out}}}{[\text{NO}]_{\text{in}} + [\text{NH}_3]_{\text{in}} - [\text{NO}]_{\text{out}} - [\text{NH}_3]_{\text{out}}}\right) \times 100\% \quad (2)$$

Assuming that the plug flow reactor (on the fixed catalyst bed) had no diffusion limitation, the NH₃-SCR reaction rate coefficient (k) over the samples was calculated by the following equation:

$$k = \left(-\frac{F_0}{[\text{NO}]_0 W}\right) \times \ln(1 - x) \quad (3)$$

where F_0 represents the molar NO feed rate (mol/s), $[\text{NO}]_0$ represents the inlet NO molar concentration (mol/mL), W_{cat} represents the weight of sample (g), and x represents NO conversion (%).

The number of atoms per unit area was calculated as follows.^[S1]

$$N_{\text{number}} = \frac{WN_A}{MA_{\text{BET}}} \quad (4)$$

where N_{number} stands for the atom number of the element per unit area, W stands for the percentage of the element, N_A represents Avogadro's constant, M represents relative the atomic mass of the element, and A_{BET} represents the BET specific surface area.

Table

Table S1 Surface/bulk atomic concentration of the VW/Ti and xMo-VW/Ti (x=1, 3, 5, 7, and 9 wt.%) catalysts.

Sample	bulk atomic concentration (wt.%) ^a		Surface atomic concentration (wt.%) ^b		The ratio of bulk atomic to surface atomic surface V/ bulk V
	V	Mo	V	Mo	
VW/Ti	0.717		0.491		0.69
1Mo-VW/Ti	0.712	1.06	0.502	1.87	0.71
3Mo-VW/Ti	0.706	2.99	0.534	2.07	0.76
5Mo-VW/Ti	0.686	5.23	0.601	3.23	0.88
7Mo-VW/Ti	0.670	7.37	0.648	5.65	0.97
9Mo-VW/Ti	0.690	10.6	0.480	6.96	0.70

^aCalculated by the ICP results.

^bCalculated by the XPS results.

Table S2 The XPS results of the VW/Ti and xMo-VW/Ti (x=1, 3, 5, 7, and 9 wt.%) catalysts for O 1s, V 2p, Mo 3d, W 4f.

Materials	O 1s		$O_{\text{ads}}/(O_{\text{ads}}+O_{\text{latt}})\%$	V 2p		$V^{4+}/(V^{4+}+V^{5+})\%$	Mo 3d		$Mo^{6+}/(Mo^{6+}+Mo^{5+})\%$	W 4f	
	BE (eV)			BE (eV)			BE (eV)			BE (eV)	
	O_{latt}	O_{ads}	V^{4+}	V^{5+}	Mo^{5+}	Mo^{6+}	W^{5+}	W^{6+}			
VW/Ti	530.2	531.4	28.0	516.2	517.2	67.2	-	-	-	35.6	36.9
1Mo-VW/Ti	530.2	531.2	28.5	516.3	517.4	68.2	231.5	232.8	73.7	35.5	36.9
3Mo-VW/Ti	530.2	531.1	28.6	516.3	517.4	70.4	231.8	232.8	74.7	35.5	36.9
5Mo-VW/Ti	530.2	531.1	29.1	516.3	517.5	71.8	232.0	232.9	75.1	35.5	36.9
7Mo-VW/Ti	530.1	531.1	29.5	516.4	517.5	73.3	232.1	232.9	80.2	35.4	36.8
9Mo-VW/Ti	530.1	531.1	25.1	516.4	517.5	71.2	232.3	232.9	77.9	35.3	36.8

Figures

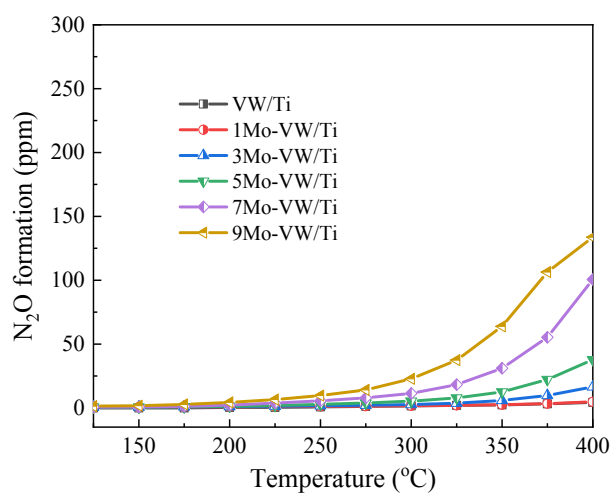


Fig. S1. N₂O formation for the NH₃-SCR activity of the VW/Ti and xMo-VW/Ti (x=1, 3, 5, 7, and 9 wt.%) catalysts.

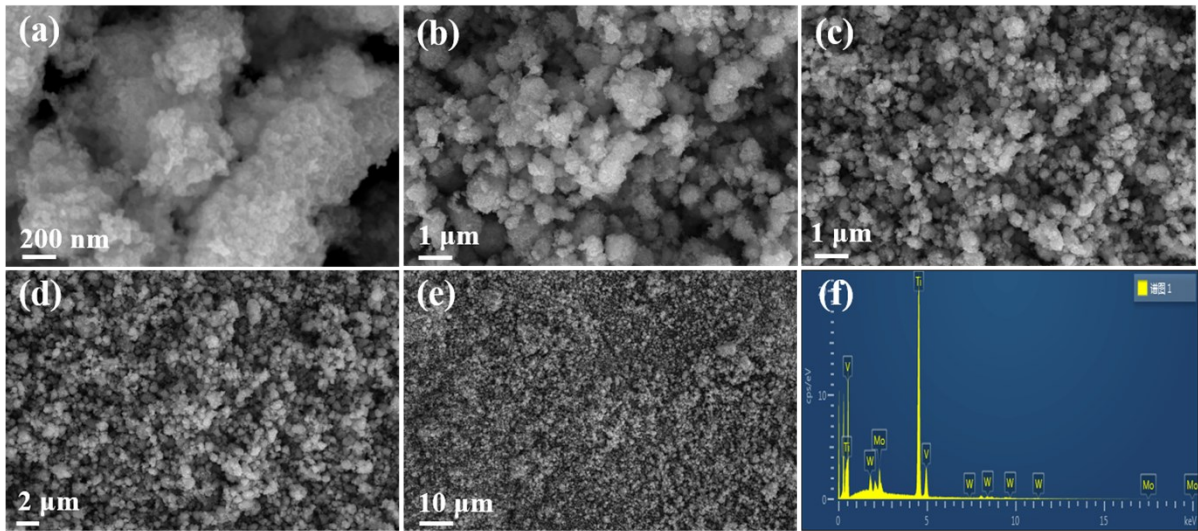


Fig. S2. (a-e) SEM images, and (f) EDX result of the 7Mo-VW/Ti catalyst.

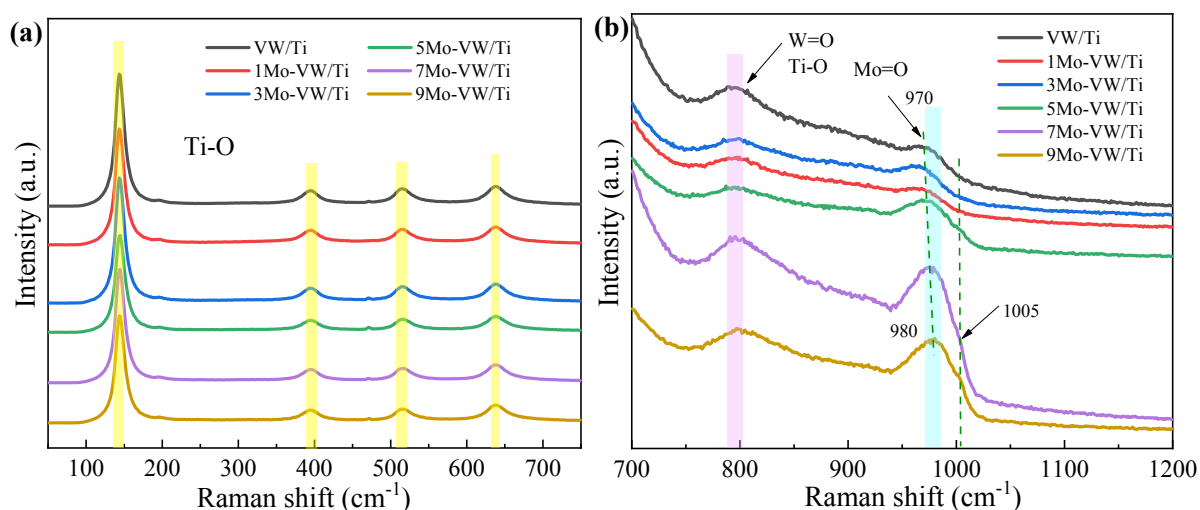


Fig. S3. Raman spectra of the VW/Ti and xMo-VW/Ti (x=1, 3, 5, 7, and 9 wt.%) catalysts at different ranges.

Raman spectra of all catalysts at different ranges are depicted in Fig. S3. In Fig. S3a, the peaks at 147 cm^{-1} , 394 cm^{-1} , 514 cm^{-1} and 636 cm^{-1} were attributed to anatase TiO_2 .^[S2,S3] Raman spectra with a narrowed high scan range of $700\text{--}1200\text{ cm}^{-1}$ are presented in Fig. S3b. The band at $\sim 800\text{ cm}^{-1}$ was ascribed to Ti-O vibration of TiO_2 or W=O stretching mode of crystalline WO_3 .^[S4-S6] According to a previous report,^[S7] the doubly coordinated oxygen O-Mo-O stretching of the broadened asymmetric band centered at approximately 819 cm^{-1} was not detected. The reasonable explanation was that little MoO_3 incorporated into the bulk phase, resulting in the formation of bulk-like MoO_3 .^[S8,S9] The band at 983 cm^{-1} was attributed to terminal Mo=O stretching.^[S10] It is obvious that the strength of the band at $970\text{--}980\text{ cm}^{-1}$ increased and the shift occurred, indicating more polymeric molybdenum oxide formed.^[S1,S10] When the loading amount of MoO_3 exceeded 7 wt.%, a weak peak of nearly 1000 cm^{-1} appeared attributed to monomeric surface vanadia or a few crystalline MoO_3 species.^[S11]

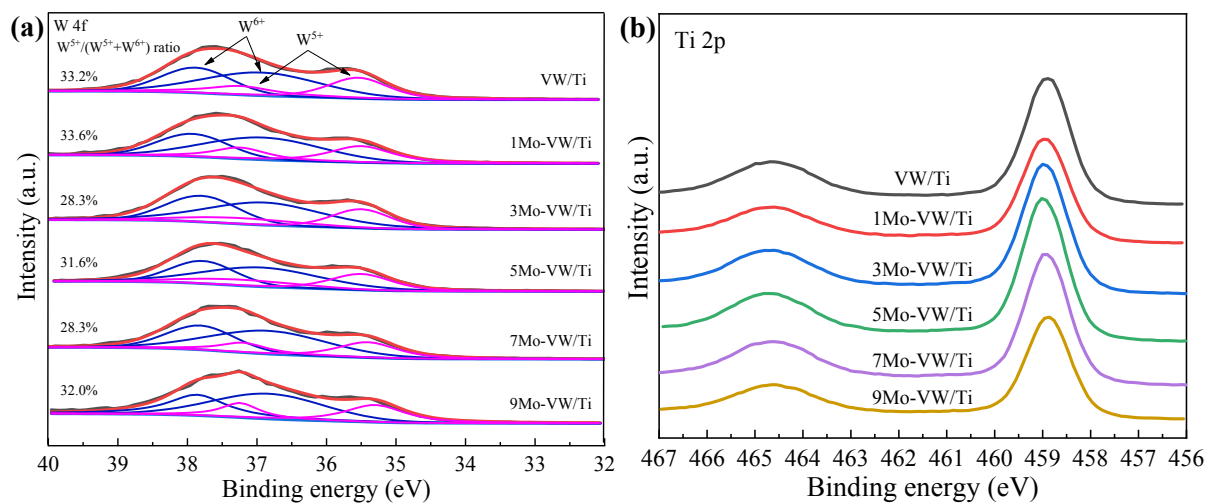


Fig. S4. XPS spectra for (a) W 4f and (b) Ti 2p of the VW/Ti and xMo-VW/Ti (x=1, 3, 5, 7, and 9 wt.%) catalysts.

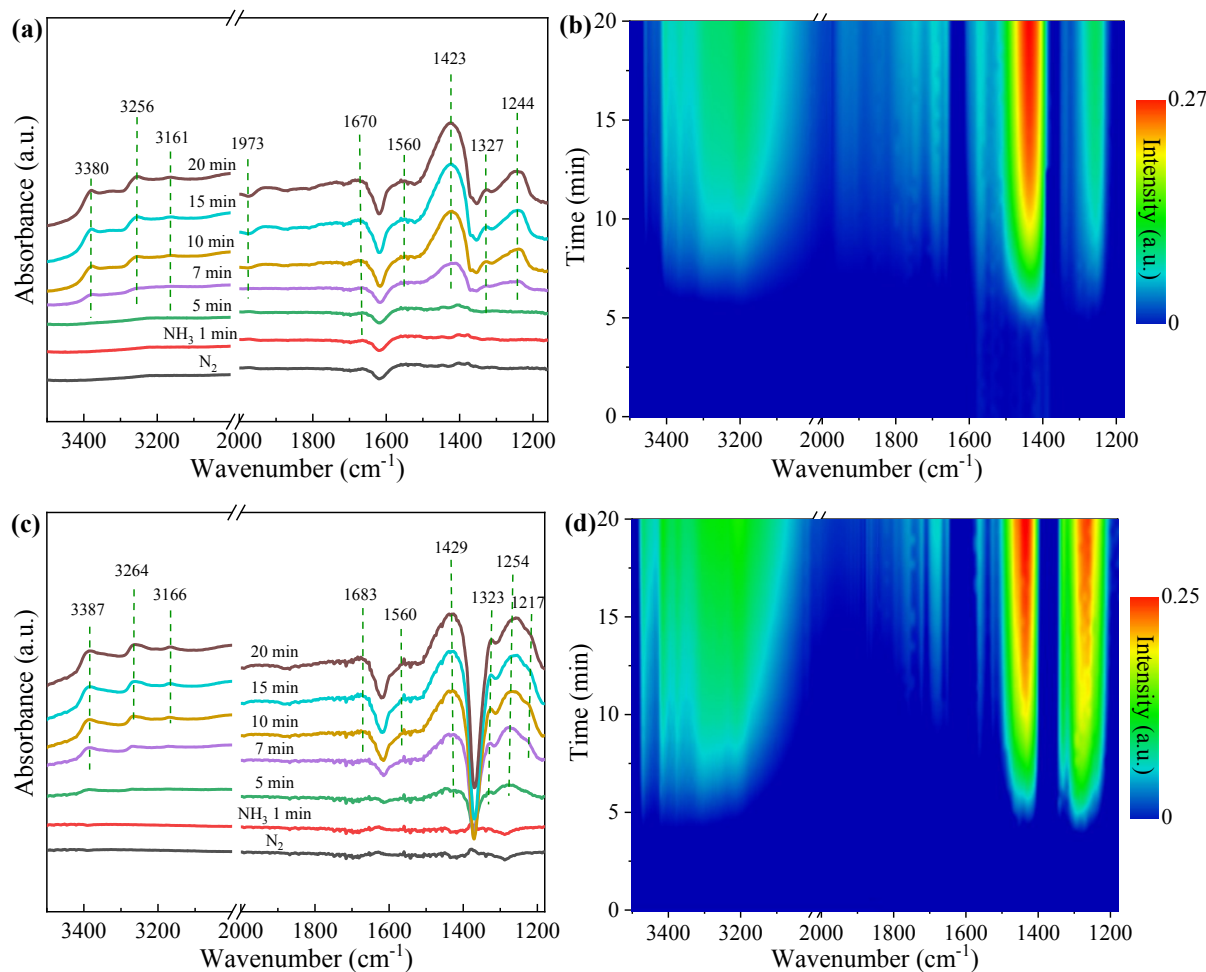


Fig. S5. *In situ* DRIFTS spectra of the (a) 7Mo-VW/Ti and (c) VW/Ti catalysts pretreated by exposure to 600 ppm NO + 6 vol.% O₂ followed by exposure to 600 ppm NH₃ at 250 °C, and the corresponding mapping of the (b) 7Mo-VW/Ti, and (d) VW/Ti catalysts.

Fig. S5 shows the *in situ* DRIFTS spectra of the reaction between pre-adsorbed NO species and gaseous NH₃ on the 7Mo-VW/Ti and VW/Ti catalysts. The changes in the profiles on both of the 7Mo-VW/Ti and VW/Ti catalyst were very similar. After NO + O₂ pretreated and N₂ purging, no obvious peaks remained on both of the catalyst surface, suggesting that the capacity of NO adsorbed on the catalyst surface was very weak. As time went on for 5 min, a large amount of NH₄⁺(B) (1670 and 1423 cm⁻¹) and NH₃(L) (3380, 3356, 3161, 1244, and 1217 cm⁻¹) species were generated. The weak bands of NH₂ amide groups (1560 and 1327 cm⁻¹) from the intermediate of ammonia oxidation were also observed. In addition, for the 7Mo-VW/Ti catalyst, molybdenyl species acted as the adsorption sites for NH₃ adsorption, so a negative peak of Mo=O bond (1973 cm⁻¹) was found because of the influence of NH₃ to unsaturated molybdenyl species.

References

- [S1] G. Dong, Y. Bai, Y. Zhang and Y. Zhao, *New J. Chem.*, 2015, **39**, 3588-3596.
- [S2] Y. Geng, X. Chen, S. Yang, F. Liu and W. Shan, *ACS Appl. Mater. Inter.*, 2017, **9**, 16952-16959.
- [S3] W. Shan, F. Liu, H. He, X. Shi and C. Zhang, *Appl. Catal. B*, 2012, **115-116**, 100-106.
- [S4] C. Wang, S. Yang, H. Chang, Y. Peng and J. Li, *Chem. Eng. J.*, 2013, **225**, 520-527.
- [S5] X. Liu, X. Wu, T. Xu, D. Weng, Z. Si and R. Ran, *Chinese J. Catal.*, 2016, **37**, 1340-1346.
- [S6] D. W. Kwon, K. H. Park and S. C. Hong, *Chem. Eng. J.*, 2016, **284**, 315-324.
- [S7] V. Jadkar, A. Pawbake, R. Waykar, A. Jadhavar, A. Mayabadi, A. Date, D. Late, H. Pathan, S. Gosavi and S. Jadkar, *J. Mater. Sci.: Mater. El.*, 2017, **28**, 15790-15796.
- [S8] R. S. Stampel, Y. Chen, J. A. Dumesic, C. Niu and C. G. Hill, *J. Catal.*, 1987, **105**, 445-454.
- [S9] Z. Huang, Y. Du, J. Zhang, X. Wu, H. Shen and G. Jing, *Environ. Sci. Technol.*, 2019, **53**, 5309-5318.
- [S10] L. Lietti, I. Nova, G. Ramis, L. Dall'Acqua, G. Busca, E. Giamello, P. Forzatti and F. Bregani, *J. Catal.*, 1999, **187**, 419-435.
- [S11] D. W. Kwon, K. H. Park, H. P. Ha and S. C. Hong, *Appl. Surf. Sci.*, 2019, **481**, 1167-1177.